Construction and Building Materials 300 (2021) 124311

Contents lists available at ScienceDirect

Construction and Building Materials

journal homepage: www.elsevier.com/locate/conbuildmat

Building pathology and environment: Weathering and decay of stone construction materials subjected to a Csa mediterranean climate laboratory simulation

Fabio Sitzia [a,b,*], Carla Lisci [a,b], José Mirão [a,b]

[a] HERCULES Laboratory, Institute for Advanced Studies and Research, University of Évora, Largo Marquês de Marialva 8, 7000-809, Évora Portugal
[b] Geosciences Department, School of Sciences and Technology, University of Évora, Rua Romão Ramalho 59, 7000-671, Évora Portugal

ARTICLE INFO

Keywords:
Ageing test
Weathering
Ultrasonic measurements
Leeb D hardness
Gas-driven permeability
μ-XRD diffraction
Hypothetical outdoor exposure

ABSTRACT

Building stone materials have to satisfy long-term durability requirements in different environments in terms of mechanical strength and resistance to aggressive conditions. Several studies and field observations show that weathering on geo-materials is related to average annual precipitation and temperature.

The decay also depends on salts air/soil concentrations and biological agents, but the more harmful impact is given by greenhouse gas (e.g. CO_2, SO_X, NO_X, O_3). These last induce the acidification of the rain and runoff waters. Nowadays, decay prediction is required in order to estimate the behaviour of stone materials over time. This research represents a second part of a previous work where the response to weathering of some construction materials used in ancient and contemporary architecture and cultural heritage has been evaluated by a laboratory simulation of hot-summer Csa Mediterranean climate. Simulation consists of accelerate ageing test on climate chamber by reproducing macro (e.g. daily and seasonal cycles of temperature, relative humidity, CO_2 air concentration) and micro (e.g. rain, soil capillary rising) environments. Some non-destructive testing were executed to evaluate some physical–mechanical "decay markers" before and after the ageing. Test caused both decreasing and increasing of Leeb D hardness, decreases of permeability and a general decrease of ultrasonic speed, mainly due to the formations of patinas, crusts and efflorescences on the surfaces.

1. Introduction

Stone materials have always been used in ancient and contemporary human settlements for building applications due to their resistance to weathering, high mechanical strength and durability. Some materials present critical problems due to their composition and textural features (e.g. carbonate, evaporitic rocks), more susceptible to chemical attack by acid/saline solutions. Nevertheless, the rock resistance, together with the aesthetic appearance, has given these building materials an enormous versatility of use. The knowledge of materials and the recognition of their pathologies are essential to define intervention strategies and mitigate the building pathologies [1].

In recent years, some damage prediction techniques have been refined thanks to accelerated ageing. This is a group of tests that simulate natural weathering by reproducing some climatic parameters (e.g. temperature, relative humidity, rain, wind, CO_2, SO_2, NaCl air concentration) that accelerate the decay processes of different materials. Ageing can consist of rapid changes of climatic conditions, aggravate high levels of stress for long/short periods, and grade of stress that certainly conduced to material breakdown [2].

Ageing tests can be divided into three typologies (quality control, qualification/validation, correlative). The first two categories consist of a short-medium test duration with fail/pass result to be compared with material specification or references imposed by the protocols [3]. Correlative tests give a rank-order data that should be compared with natural exposure [4]. Ageing on building materials dedicate to the quality control, express the damage in terms of material weight loss and must fall within a certain range of values acceptable for a specific use. The building materials ageing is mainly regulated by normative as:

UNI EN 13919:2004 [5], UNI EN 12370:2001 [6], UNI EN 14066:2013 [7], UNI EN 14147:2007 [8] and UNI EN 12371:2010 [9]. Recently, accelerate ageing by condensation, saline and sulphuric fog for polymers, metals and automotive (e.g. DIN 50,017 [10], DIN 50,018 [11], DIN 50,021 [12], ISO 9227:2017 [13] and ASTM G154 C.7 [14])

* Corresponding author.
E-mail address: fasitzia@tiscali.it (F. Sitzia).

https://doi.org/10.1016/j.conbuildmat.2021.124311
Received 24 March 2021; Received in revised form 15 June 2021; Accepted 19 July 2021
Available online 26 July 2021

have also been handled on construction and building materials.

Some of the tests mentioned above submit the samples to high-stress levels for short periods by the "aggravation practice". For instance, the temperature of + 105 °C, −20 °C, Na_2SO_4 saline solutions at 14% concentration and SO_2 aggressive atmosphere > 5 ppm are recommended by normative."Aggravation practice ageing" has been performed by researchers, identifying a general deteriorating of physical–mechanical parameters and chemical decay. According to other reseraches [15], the ageing test on building stone materials by Freeze - Thaw (F-T) and Heating - Cooling cycles (H-C) causes an overall decrease of P-wave velocity and uniaxial compressive strength. This is due to micro-fractures created by the expansion of the ice inside the rock porous system. Decreases of P-wave velocity after F-T cycles have been evaluate [16] together with a decrease of uniaxial compressive, tensile, point load and block punch index (BPI). An experiment conducted on andesites used as building stone in Turkey [17], identified how F-T cycles induce an increasing of Böhme abrasion loss (BA). It has been detected how ageing also determined a loss of weight due to different typologies of decay. Some authors [18], suggest that degradation of limestones are linked to the strong thermal expansion anisotropy of calcite crystals, which produce, simultaneously, detachments and stresses on grain edges. The aggravation practice of F-T and H-C tests not only generate a worsening of the most common features but also the variation of other proprieties as the Shore hardness [19], J.R.C. roughness [20], and pore connectivity/tortuosity [21].

Ageing by corrosive and saline atmosphere aims to simulate marine aerosol or anthropic pollution of urban settlement. The saline fog by UNI EN 14147:2007 brings the increase of microfractures in sandstones as results of salt crystallization inside the porous network [22].

The aggravation practice test presents a lot of chancy due, for example, to the different chemical/physical processes that evolve at extreme temperatures/relative humidity respect than real ones. Besides, different chemical compounds could be formed in a high concentrated SO_2 or CO_2 ageing atmosphere compared to those of the real (and realistic) environmental concentrations.

A partial alternative to the "aggravation practice test" with "real simulation practice test" is recently proposed. Cycles of temperature, relative humidity and other parameters simulate the day, night and seasons in a few minutes. The main goal of "real simulation practice test" is to recreate a certain climatic context and verify the degree of weathering on tested materials in a reliable and realistic way. Some authors [23] have realized a hybrid ageing subjecting cement and mortars to some F-T cycles according to ASTM D5312 standards, but using the average max. and min. temperatures of Northern Portugal, instead of + 20 °C and −20 °C required by the standard. The durability of lime mortars was also tested by subjecting samples to max. temperature, relative humidity and Na_2SO_4 aerosol deposition typical of Granada (Spain) [24].

Other weather circumstances as insolation, rain and frost were simulated on sandstones to reproduce the continental climatic conditions (e.g. humid continental (Dfb), temperate oceanic (Cfb) [25]) of S-W Poland [26]. Ageing consisted of a rotating chamber with 24 h cycle exposing the sample to rain at 16 °C, followed by a thawing at 70 °C to simulate the exposition to sun. A subsequent exposition to −20 °C models the rigid winter condition of Poland. The authors also determined the variations of porosity, hysteresis and threshold diameter with the help of Hg porometer (MIP).

Continental climatic simulation of Czech Republic (temperate oceanic climate [25]) in terms of F-T cycles, was carried out [27], consisted of a combination of experimental analysis and numerical climate simulation for evaluating the service life of sandstone used in Cultural Heritage.

In 2013, Bochen [28] conducted an accelerated ageing test on building components (e.g. thin layered plasters, façade insulation systems, cellar concrete) in climatic chamber. This consisted of central rotating chamber sides by a sun chamber, a wind/rain chamber and a frost chamber. A complete cycle of 4 × 50 min exposed the samples to solar radiation (400–700 nm wavelength at 75 °C temperature), rain, wind and frost at −25 °C. Based on the analogy between characteristic simulate climate (CSC) and Katowice-Muchowiec meteorological station, the test has been calibrated for reproducing 2.5 years of natural outdoor exposure in Silesian climate with 100 cycles.

Other weathering in a complex climatic chamber (CIME) was performed by some authors [29] to mimick the interactions between Cultural Heritage materials and environmental parameters as: temperature, relative humidity, solar radiation, gaseous pollutants and different types of particulate matter such as terrigenous, marine and anthropogenic. The test had the capacity to simulate a marine and/or urban environment.

A salt weathering on schist in line with realistic field parameters have been carried out [30]. The experiment, in this case, evaluates the decay degree and amount of decohesion residue for the prediction of the landform evolution over time. Furthermore, a mining waste environment of Australia has been reproduced in laboratory with salt solution of $MgSO_4$ as observed on *in situ* runoff water. In addition to the wetting, a simulation of T and rH of daily dry and wet season temperature profiles occurred.

In the affinity of "real simulation practice", this research represents the second part of a project started in 2021 [31] with the aim of investigating the durability of stones exposed to Mediterranean hot summer (Csa) climate.

The authors identified a wide range of pathologies due to weathering during *in situ* observations on ancient monuments of Sardinia Cultural Heritage (Italy). The research questions of the project are two:

i) is it possible to recreate in the laboratory all the observed building materials pathologies by simulating the environment and the climatic context where the buildings are located?

ii) is this simulation reliable and predictive?

To address this issues, two simulations of micro and macro environment were associated and occurred on samples of building stone materials of the four most important monuments of Sardinia. A macro-reconstruction of monument environment condition was done by simulating the trends of daily and seasonal variations of temperature, relative humidity, and CO_2 air concentration according to the real parameters acquired from meteorological Sardinia databases. These last ones indicated a mild climate classified as hot-Mediterranean (Csa) [25]. A micro-reconstruction was done in order to simulate micro-environment context (e.g. rain and soil capillary rising) of a specific spot of the monuments.

As displayed in the previous work [31], ageing on stone materials caused a slight alteration, mainly identified by a loss of weight for stone decohesion. Degradation of samples also caused some morphological changes due to exfoliation, differential erosion, detachments and a decrease of point load strength index.

In addition to the associated reproduction of macro and micro environmental contexts, the research presented some innovative features as:

a) The faithful reproduction of capillary rising by using saline solutions not prepared in laboratory but collected *in situ*.

b) The possibility to evaluate the morphological changes on the samples before and after the ageing by 3D modelling.

In this second part of the research, others non-destructive testings (NDT) as Leeb D hardness, gas-driven permeability, ultrasonic pulse speed and efflorescences analysis will be shown for defining a complete picture about the behaviour of stone subjected to accelerate ageing.

The real simulation ageing affords crucial disclosure about the base-principle of geo-materials decay, durability, aesthetic features changing and could be manage to predict some strategic implications in the field of stone conservation. In fact, this test can also work on mortar, putty, concrete or asphalt, protective and consolidating treatments for addressing the material to a certain indented of use in a specific climatic context.

2. Materials and methods

2.1. Materials

Considering their variability and importance in the Sardinia monuments, the analysed stones were Tyrrhenian Sandstone, biomicrite, biolitite, basalt, Carrara marble, rhyodacite, and two chromatic *facies* rhyolites. Two samples, measuring 50x50x50mm ± 5 mm, of each stone were cut. This lithologies belongs to four case-study historical monuments of Sardinia (e.g., *Forum Traiani* baths, San Saturnino Basilica, buildings of *Tharros* archaeological area and *Nora* Theatre, Table 1). The stones were collected into ancient quarries, identified by bibliography, geochemical-petrographic and isotope-ratio data between monument and outcrops materials were compared [20,32–35].

With the purpose of simulating the effect of the macro-environment of monument location, all cubic samples of 50x50x50mm ± 5 mm dimension have been subjected to T and rH cycles, in a stable CO_2 concentration atmosphere (see methods).

For simulating small-scale micro-environments, for each lithology, a sample was subjected to capillary rising test with saline water (C_{GW}, C_{SW} and C_{TW}) and the other with rainwater (C_{RW}). Capillary rising test by saline waters simulates the conditions in the basal part of the monuments in contact with damp soil. In particular, capillary rising with groundwater (C_{GW}) collected in the aquifer below San Saturnino Basilica, simulates on biomicrites, biolitites and marble the process of aquifer rising humidity that starts from the building foundations and reaches several meters high, sometimes flooding the crypt and wetting the areas of transept (Fig. 1a).

Capillary rising seawater (C_{SW}) on basalts, Tyrrhenian sandstones and rhyodacites simulate the sea spray deposition on walls structures of *Tharros* archaeological area (Fig. 1b) and *Nora* theatre located closed to coastline. At *Nora* theatre especially, morphological irregularity in the step treads favoured the accumulation of meteoric water, salinized by the marine spray from the south quarters wind (Fig. 1c).

Capillary rising with thermal waters (C_{TW}) on rhyolites simulate the micro-environmental of the external bathtubs present in the ancient thermal system of *Forum Traiani* (Fig. 1d) where a source of natural spring waters is still present [36].

Capillary rising with rainwater (C_{RW}) simulates the wetting due to the rain on all selected samples.

In Table 2, the hydro-geochemical analysis and other features as total dissolved solids (TDS), temperature and pH of the waters used for capillary rising tests, togheter with the amount of ions dissolved in the solutions are present.

2.2. Methods

As shown in the previous work [31], temperature, relative humidity and CO_2 air concentration were simulated by climatic chamber ARALAB FITOCLIMA S600PLH with FITOLOG 600 control software.

The maximum, minimum and the trends of temperature (T) and humidity (rH) of the monument locations (Table 3) were obtained from the Italian Air Force and Italian Civil Aviation Authority (http://clima.meteoam.it/AtlanteClimatico).

In FITOCLIMA chamber, a daily T and rH trends was reproduced in 40 min of test and a season in 3600 min.

In 6 months of test duration, samples underwent to 1.5 months of winter, 1.5 springtime, 1.5 summer and 1.5 autumn according to the trends show on the previous work [31].

During ageing on FITOCLIMA chamber, capillary rising tests have been conducted by applying 12 ml of water to every sample, once every 24 h. The base of each sample was immerse in a pool of water with 3 mm deep allowed it to dry out over time.

Ageing has been conducted with a realistic Sardinia CO_2 air concentration of 403 ppm according to GIOVANNI database (https://giovanni.gsfc.nasa.gov/giovanni).

The test was designed with a duration of 6 months mainly for two reasons: it was observed how some physical–mechanical and chemical characteristics of the stone rapidly vary in the first weeks of testing tending to stabilize over time. The formation of the efflorescences took about 2 months from the test beginning to the moment they could be macroscopically observed.

For μ-XRD analyses of efflorescences, a Bruker AXS D8 Discover XRD with a CuKα source, operating at 40 kV and 40 mA, and a Lynxeye 1-dimensional detector was used. Scans were performed from 3 to 75°2θ, with 0.05°2θ step and 1 s/step measuring time by point. Diffract-Eva software from Bruker with PDF-2 mineralogical database (International Centre for Diffraction Data - ICDD) was utilized to interpret the scans. During the μ-XRD experiments, a Goebel mirror and 1 mm collimator was employed.

Measurements of the P waves speed (Vp) were carried out using PUNDIT PL200 PROCEQ with transducers of 2.8 cm diameter and frequency 250 kHz; coupling material: silicone. For every sample, Vp speed expressed in m/s has been measured in X,Y and Z direction. The velocity ratio quality index (VRI) indicates the stone quality based on the ultrasonic velocity measurements in building and in quarry. VRI is calculated as $(Vp_{in\ situ}/V_r)^{0.5}$ where $Vp_{in\ situ}$ is the ultrasonic Vp speed measured on building and Vr is the value of intact quarry rock [37].

For our propose, VRI has been calculated as:

$VRI = (Vp_{post\ test} / Vp_{pre\ test})^{0.5}$ assuming that $Vp_{in\ situ}$ is the post test Vp value (ageing happened on buildings for a hypothetical outdoor exposition of about 18 years) and V_r is the value of $Vp_{pre\ test}$ or rather the ultrasonic speed of quarry materials.

For hardness measurement, a portable hardness tester Leeb D EQUOTIP (Proceq), with wireless software platform EQUOTIP LIVE has been used. Instruments is indirect verified, according to ISO16859-2 normative [38]. The calibration data was 767.33 ± 2.51 HLD for metal block B face and 768.33 ± 3.05 HLD for A face.

During the measuring by Leeb D a 1.5 mm radius penetrator impacts on the sample surface with kinetic impact energy of 11.5 mJ. The HLD index is calculated as $= (v_r/v_i)1000$ where v_r is the rebound velocity (0.615–1.8245 m/s) and v_i is the penetrator velocity (2.05 m/s, data from Proceq).

The gas-driven permeability was measured by handheld air permeameter TINY PERM 3 with NER-supplied Android wireless storing data software. Both gas-driven permeability and Leeb D hardness were only one time measured before and after ageing at the centre of every face composing the cubic 50x50x50mm ± 5 mm specimens. Single impact method (SIM) was performed.

The 3D specimen models were performed by using the photogrammetry software Agisoft Photoscan 1.4.4. For the reconstruction, a Nikon D3300 camera (24Mpx resolution) with 18–50 mm f / 3.5–5.6 DC D was used. A total of 90 photos per sample were taken by building the upper and the lower half (chunks) of the model, subsequently combined using

Table 1
Case study monuments (Sardinia, Italy) and building stones type.

Monument	Geographical coordinates	Municipality location	Age (Cent. AD)	Architectural style	Stone building material
Forum Traiani baths	39°59′49,19′′N 8°48′30,16′′E	Fordongianus	I-IV	Roman	Rhyolites (red and green *facies*)
San Saturnino Basilica	39°12′49,77′′N 9°07′23,73′′E	Cagliari	IV-XII	Roman, Romanesque	Carrara marble, biomicrite, biolitite
Tharros buildings	39°52′24,30′′N 8°26′27,73′′E	Cabras	II	Roman	Basalt, sandstone
Nora theatre	38°59′03,93′′N 9°00′59,26′′E	Pula	III	Roman, Phoenician-Punic	Rhyodacite

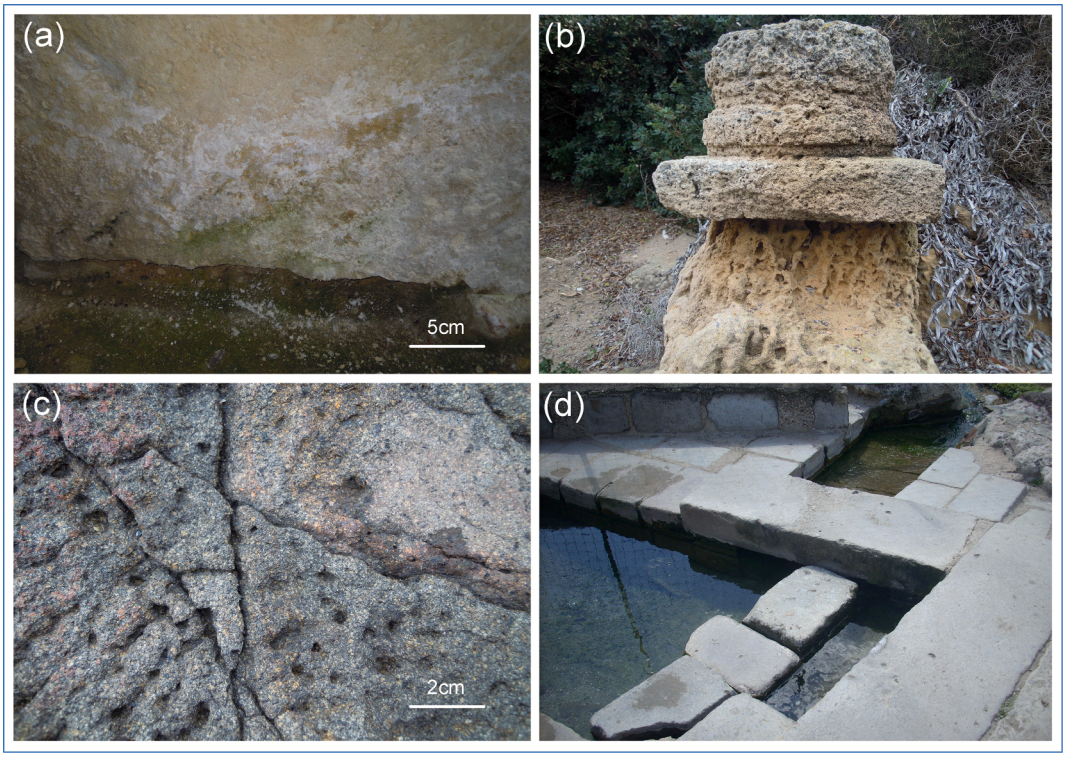

Fig. 1. (a) capillary rising of groundwater and efflorescences formation in the area of transept (San Saturnino Basilica), (b) granular decohesion and erosion on a sandstone Roman column due to marine spray, (c) irregularity of rhyodacites surface, (d) rhyolites in contact with thermal water (T = 52.1 °C) at *Forum Traiani* archaeological area.

Table 2
Hydro-geochemical and physical /chemical characteristics of waters used for capillary rising tests at the moment of sampling.

Collected water	TDS (mg/l)	Temperature (°C)	pH	Conductivity (μS/cm)	Mg^{+2} (mg/l)	Na^{+} (mg/l)	K^{+} (mg/l)	Ca^{2+} (mg/l)	Cl^{-} (mg/l)	SO_4^{-2} (mg/l)	HCO_3^{-} (mg/l)
Ground water (C_{GW})	491	13.0	8.1	980	12	68	9	28	174	35	104
Seawater (C_{SW})	37,330	17.8	7.9	N/A	1450	10,010	427	408	19,950	3000	179
Thermal water (C_{TW})	826	52.1	8.6	1652	4	200	202	45	306	50	N/A
Rainwater (C_{RW})	42	11.8	6.5	84	1	3	1	10	5	4	12

Table 3
Climatic data of monument.

Average Min, Max temperature and humidity of monument location	Season			
	Winter	Springtime	Summer	Autumn
Max. average temp. (°C)	14.2	18.4	28.3	22.3
Min. average temp. (°C)	7.0	10.2	18.9	14.3
Max. average relative humidity (%)	91	84	78	83
Min. average relative humidity (%)	71	70	66	73

4/5 paper targets applied on the specimen. Total dissolved solids, temperature, pH and conductivity of capillary rising waters have been measured with the help of a PANCELLENT TDS&ECmeter and pHmeter. For hydrogeochemical analysis, the samples were *in situ* stabilized by high-purity acid with 1% HNO_3. Anion species were determined by ionic chromatography and ion selective electrode on filtered and unacidified waters. Analysis of the metals has been done by atomic absorption spectroscopy (AAS), graphite furnace atomic absorption spectroscopy (GFAAS), and inductively coupled plasma optical emission spectroscopy (ICP-OES)

2.3. The concept of hypothetical outdoor exposure

The total period of ageing test on FITOCLIMA climatic chamber is 6 months ($T_T = 2.592 \bullet 10^5$ min). Considering that an accelerate daily cycle has been done in 40 min, a total of 6480 daily cycles were reproduced, corresponding to about 18 years of hypothetical outdoor exposure (T_A, acceleration factor F = 36). As indicated in the previous work [29], the term hypothetical outdoor exposure, introduced by [31], indicates a incertain correspondence between the decay reproduced in six months of test and 18 years of natural outdoor exposure (T_{NA}). This happens due to several issues as:

1) the high complexity of natural weathering
2) the ageing test design

Even if authors try to faithfully mimic some climate parameters in laboratory, the discrepancy between artificial ageing and natural weathering comes, for instance, from:

i) The speed of the artificial ageing processes: different deterioration occurs in climatic chamber due to the short-term of the process respect than long-term of natural outdoor exposure [39,40].

ii) The existence of extreme climate events: some climatic parameters as temperature and relative humidity have been set according to average data of 30-years period (1971–2000) without taking into

account extreme events (e.g. T < 0 °C, T = 45 °C) that are considered most dangerous for the breakdown of the stone matrix.

iii) The contribution of other decay agents acting in outdoor environment: parameters not regulated on climatic chamber but present in natural exposure as: the orientation of the samples to rain, wind or sun main directions, bio-deterioration, dirty and solid combustion product deposits that react with stones.

Differences between natural and artificial exposure can be detected in the ageing test design, especially regarding the cycle duration and the accelerator factor. An over-accelerate ageing with, for instance, very short cycles of T, rH and consequently, high acceleration factors, must be avoided [3]. Materials placed in the climatic chamber should have the ability to balance their temperature and humidity with the external environment. Otherwise, the steady-state is not reached and weak variations of T and rH occurs only in the superficial layers. Researchers declare that an accelerator factor of 30–40 (36 in our case) can be considered acceptable [28].

For this reason, if we want to consider our accelerate ageing decay, as correlative test in terms of physical, mechanical, chemical and geometric features, the same ones must be monitored and verified in natural outdoor exposure. In literature, some example of monitoring on long-term natural exposure have been execute during 9 years on ceramics [41], on facing and roofing at the Building Research Institute in Warsaw [42] and on masonry coating-systems [43].

3. Results and discussions

3.1. Interaction between capillary rising waters and stones

After 6 months of accelerated ageing, corresponding to a hypothetical outdoor exposure of ≈18 years, efflorescences on cubic samples were identified by μ-XRD technique (Table 4). The efflorescences are well visible on post ageing 3D models of the samples available at the links reported in Table 5 and in Fig. 2.

Efflorescences are mainly located at the lower part of samples above the water film, so in the rising dump front (stall-line) well visible, for example, on basalts (Fig. 2d).

As illustrated in Table 4, halite (NaCl) is detected on the sandstone AT2 subjected to capillary rising with seawater. Other phases as calcite, quartz and plagioclase belong to the original stone, were just identified by optical microscopy in the previous work [31]. On biomicrites, from 2% up to 40% Wt. of gypsum ($CaSO_4{\cdot}2H_2O$) has been detected on both samples. Gypsum and halite on PC2 sample probably results from a sulphating calcium carbonate process due to interaction with salts-rich groundwater (Table 2). For this purpose, it has been displayed as Cagliari aquifer is subjected to two main contaminations: i) infiltration of wastewater from sewerage system and cesspit, ii) seawater intrusion due to the overexploitation of groundwater for domestic and industrial purposes [44].

Table 5
Links to 3D digital models after and post ageing. T = temperature, rH = relative humidity, CO_2 = carbon dioxide air concentration, C_{RW} = capillary rising with rainwater, C_{SW} = capillary rising with seawater, C_{GW} = capillary rising with groundwater, C_{TW} = capillary rising with thermal water.

Sample	Lithology	Reproduced conditions	3D online models by photogrammetry	
			Pre test (T_T = 0 days)	Post test (T_T = 180 days)
AT1	Sandstone	T, rH, CO_2, C_{RW}	https://bit.ly/2EBZ4wn	https://bit.ly/38YukDR
AT2		T, rH, CO_2, C_{SW}	https://bit.ly/34HyTio	https://bit.ly/2PEtPHr
PC1	Biomicrite	T, rH, CO_2, C_{RW}	https://bit.ly/38Ys2EL	https://bit.ly/2PGuM1V
PC2		T, rH, CO_2, C_{GW}	https://bit.ly/2SbzeYc	https://bit.ly/35LGaiI
PF1	Biolitite	T, rH, CO_2, C_{GW}	https://bit.ly/35JvrVX	https://bit.ly/36W8qiR
PF2		T, rH, CO_2, C_{RW}	https://bit.ly/2Mc0JwP	https://bit.ly/2SagyYL
MA1	Marble	T, rH, CO_2, C_{GW}	N/A	N/A
MA2		T, rH, CO_2, C_{RW}	N/A	N/A
BA1	Basalt	T, rH, CO_2, C_{SW}	https://bit.ly/38ZYS8r	https://bit.ly/2Q4SmV7
BA2		T, rH, CO_2, C_{RW}	https://bit.ly/38UmHOZ	https://bit.ly/390C0W3
AN1	Rhyodacite	T, rH, CO_2, C_{SW}	https://bit.ly/2s5WAnt	https://bit.ly/2rXvIGn
AN2		T, rH, CO_2, C_{RW}	https://bit.ly/38Rfn6u	https://bit.ly/2ZbpAGl
IGv1	Rhyolite green *facies*	T, rH, CO_2, C_{TW}	https://bit.ly/2Z7Hw4O	https://bit.ly/35G3PB2
IGv2		T, rH, CO_2, C_{RW}	https://bit.ly/2Mc1juv	https://bit.ly/2reopcX
IGr1	Rhyolite red *facies*	T, rH, CO_2, C_{TW}	https://bit.ly/36Q9BA8	https://bit.ly/2EE263j
IGr2		T, rH, CO_2, C_{RW}	https://bit.ly/2SclJYh	https://bit.ly/2EzQONF

N/A = not available, photogrammetry cannot be done on crystalline rocks.

Table 4
Results of μ-XRD diffraction on efflorescences detected after aging.

Sample	Lithology	Reproduced conditions	Cal	Qtz	Pla	Kf	Mus	Gy	Ha	Dio	Oli	Tit	Ens	Blo	Eps	Ru	Mag
AT1	Sandstone	T, rH, CO_2, C_{RW}	••	•••	•	–	–	–	–	–	–	–	–	–	–	–	–
AT2		T, rH, CO_2, C_{SW}	•	•••	••	–	–	–	•	–	–	–	–	–	–	–	–
PC1	Biomicrite	T, rH, CO_2, C_{RW}	•••	Tr	–	–	–	•	–	–	–	–	–	–	•	–	–
PC2		T, rH, CO_2, C_{GW}	•••	–	–	–	–	•••	Tr	–	–	–	–	–	•	–	–
PF1	Biolitite	T, rH, CO_2, C_{GW}	•••	–	•	–	–	–	•	–	–	–	–	–	–	–	–
PF2		T, rH, CO_2, C_{RW}	•••	–	Tr	–	–	–	–	–	–	–	–	–	–	–	–
MA1	Marble	T, rH, CO_2, C_{GW}	•••	–	•	–	–	••	••	–	–	–	–	–	–	–	–
MA2		T, rH, CO_2, C_{RW}	•••	–	•	–	••	•	–	–	–	–	–	–	–	Tr	–
BA1	Basalt	T, rH, CO_2, C_{SW}	–	–	•••	–	–	••	–	–	•	–	–	–	–	–	–
BA2		T, rH, CO_2, C_{RW}	–	–	•••	••	–	–	–	–	–	•	–	–	–	–	–
AN1	Rhyodacite	T, rH, CO_2, C_{SW}	–	•	•••	–	–	•••	•	–	–	–	–	–	–	–	–
AN2		T, rH, CO_2, C_{RW}	–	–	–	–	–	Tr	–	••	–	–	–	–	–	–	•
IGv1	Green *facies* rhyolite	T, rH, CO_2, C_{TW}	–	••	••	••	–	–	–	–	–	–	–	••	–	–	–
IGv2		T, rH, CO_2, C_{RW}	–	••	••	••	••	–	–	–	–	–	–	–	–	–	–
IGr1	Red *facies* rhyolite	T, rH, CO_2, C_{TW}	–	••	•••	••	–	–	–	–	–	–	–	–	–	–	–
IGr2		T, rH, CO_2, C_{RW}	–	••	••	••	–	–	–	–	–	–	••	–	–	–	–

Cal = calcite, Qtz = quartz, Pla = plagioclase, Kf = potassium feldspar, Mus = muscovite, Gy = gypsum, Ha = halite, Dio = diopside, Oli = olivine, Tit = titanite, Ens = enstatite, Blo = bloedite, Eps = epsomite, Ru = rutile, Mag = magnetite.
Tr = traces (≤2% Wt.), • = present (2–10% Wt.), •• = abundant (10–40% Wt.), ••• = very abundant (≥40% Wt.).
T = temperature, rH = relative humidity, CO_2 = carbon dioxide air concentration, C_{RW} = capillary rising with rainwater, C_{SW} = capillary rising with seawater, C_{GW} = capillary rising with groundwater, C_{TW} = capillary rising with thermal water.

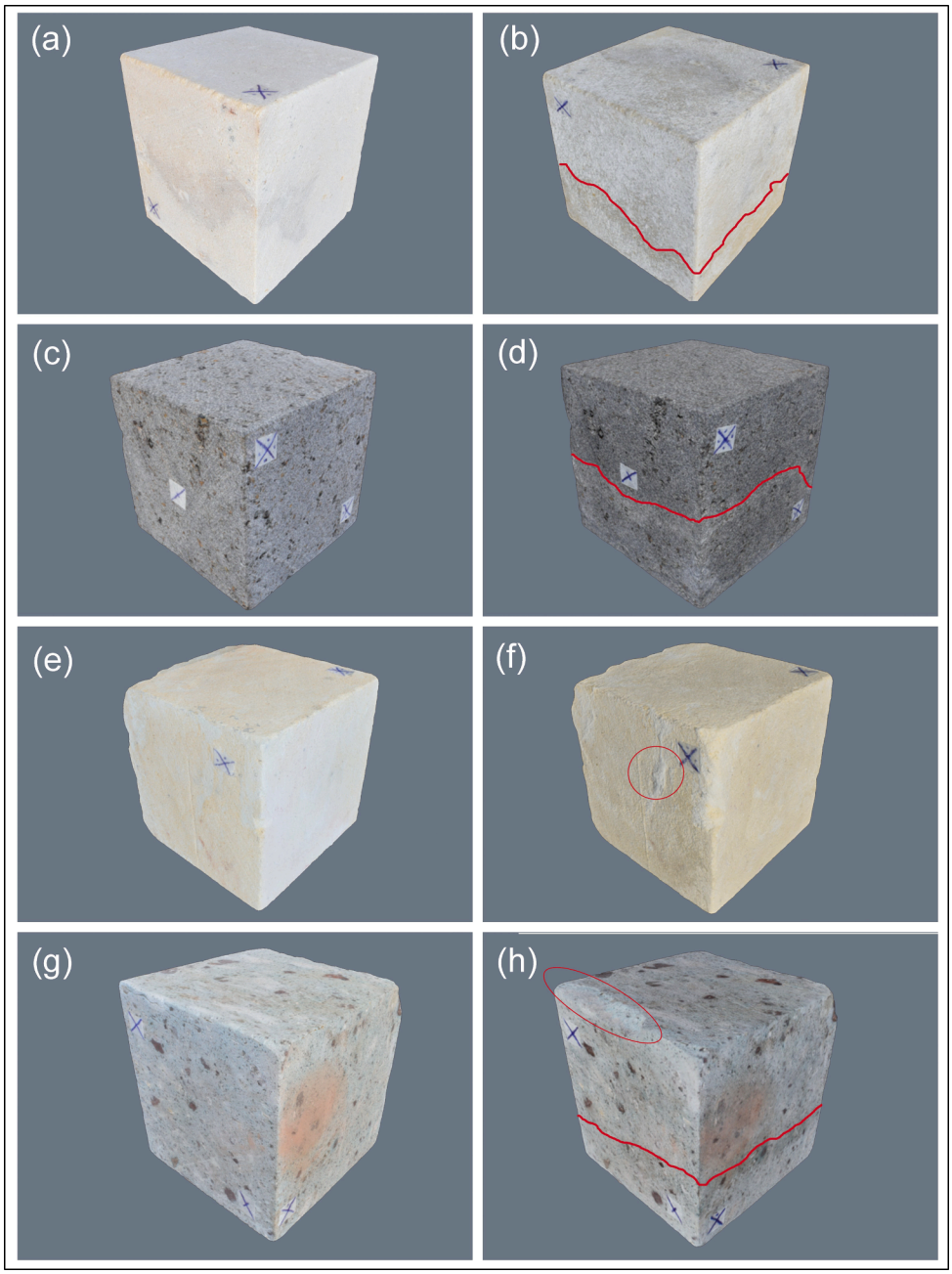

Fig. 2. (a) sample PF1 pre test, (b) sample PF1 post test, the rising dump front of capillary rising is well visible and identified with the red line. Sample is covered by white efflorescences, (c) sample BA1 pre test, (d) sample PF1 post test, the rising dump front of capillary rising is well visible and identified with the red line. White saline deposition are present in correspondence with the red line, (e) sample PC2 pre test, (f) sample PC2 post test. A crack due to material decohesion is identified with the red circle, (g) sample IGv2 pre test, (h) sample IGv2 post test. The rising dump front of capillary rising is well visible and identified with the red line. A principle of exfoliation decay is indicates with the red ellipse. (For interpretation of the references to colour in this figure legend, the reader is referred to the web version of this article.)

In addition, some gypsum could be already present at the moment of sampling due to a sulphating process in outcrop. Gypsum could be a product of reaction between $CaCO_3$ from the rock and from SO_4^{2} anion presents in rainwater, in this case 7.3 mg/l (Table 2). This explains the presence of gypsum on PC1 sample only affected by rainwater.

Epsomite ($MgSO_4 \cdot 7H_2O$) is detected both on PC1 and PC2 in association with gypsum efflorescences as visible in the models of Table 5 and Fig. 2e, f. Epsomite is an evaporitic mineral that, in this case, develops from the sulphating process of Mg-bearing carbonates. The thin-sections of biomicrites, as shown by some authors [20,33], exhibits a rich fossil fauna represented by magnesium calcite $(Ca,Mg)CO_3$ skeleton (e.g. echinoderms, [45]). Epsomite has an extreme solubility and ionic mobility, in the presence of aqueous solutions and can penetrate in the matrix and then recrystallize during the subsequent evaporation phase [46]. Sulphate efflorescences (e.g. mirabilite, thenardite) have also been detected on biomicrites inside the church of San Saturnino (area of transept) [47]. On biomicrites, calcite, quartz and plagioclase are attributable to the carbonate substrate and allochems minerals.

On biolitites, efflorescence of NaCl (i.e. halite) has been detected on PC1 sample subject to capillary rising with groundwater.

On marbles, phases as calcite, plagioclase, muscovite and rutile coming from the rock substrate were detected in agreement to the results of [31,32]. Gypsum efflorescences are detected on both marble samples due to a sulphating of calcium carbonate substrate. A large amount of halite is detected on MA1 subjected to capillary rising with groundwater. This, again, confirms that groundwater is partially present a sodium-chloride hydro-geochemical *facies* (Table 2) also due to the short distance ($\approx$ 670 m) to the actual coastline and an elevation of $\approx$ 10 m a.s.l.

On basalts, gypsum is detected on BA1 sample and probably derives also from seawater reacting with a Ca-bearing rocks.

White gypsum efflorescence on BA1 are well visible in the models of Tale 5 and Fig. 2c, d).

According to Murgia (2014) [48], in fact, basalts of *Tharros* area

present a content of CaO between 5 and 8% wt.

On rhyolites, efflorescences of bloedite $Na_2Mg(SO_4)_2{\cdot}4H_2O$ are detected on IGv1.

This mineral phase is typical of evaporitic deposits. It can be detected as crust salt evaporation in the soil due to leaching by rainwater [49]. In our case, bloedite is probably due to precipitation from thermal water used in capillary rising tests.

Forum Traiani thermal waters present sodium chloride and sulphurous hydro-geochemical *facies* as shows in Table 2. The characteristics of this water were already detected in a old research [50]. Another study [36] showed as the water of *Forum Traiani* sources reacts with the mortars of the archaeological site by the formation of harmful hydrocalumite ($Ca_2Al(OH)_{6.5}Cl_{0.5}{\cdot}3H_2O$). The salt deposition founded in the stones (Table 4) have been compared with RUNSALT software [51,52] a graphical user interface to the ECOS thermodynamic model for the prediction of the behavior of salt mixtures under changing climate conditions.

The results were enough similar. As indicated in the software, groundwater with its composition (Table 3) involves the precipitation of gypsum and halite based on the relative temperatures and humidity set in the climatic chamber for all the seasons. These two minerals were found in the stones affected by groundwater (Table 4).

The same products of precipitation (gypsum and alite) were predicted by RUNSALT and found in the stone affected by seawater (Table 4).

About thermal water, some discrepancies have been found between simulation and real data. Table 4 reports the presence of Bloedite on rhyolites not predicted by the software. Contrary, RUNSALT predicts the precipitation of sylvite KCl and Gorgeyite $K_2Ca_5(SO_4)_6{\cdot}H_2O$ not detected by XRD due to the high content of K into the thermal water (Table 3).

Rainwater produced deposition of gypsum as detected on Table 4 and predicted by the software.

3.2. Ultrasonic measurements

Table 6 exhibits the speed of Vp longitudinal pulse in the samples before and after the ageing test. A general decrease of the speed occurs in all the samples. As demonstrated in the first part of the work [31], the alteration is especially located at the most superficial layer, where the salt pressure crystallization leads to a general increase of the open porosity. Cyclic salt crystallization and solubilization, weakly reduce the mechanical resistance of the rocks as confirmed by the decrease of point load and compressive strength [31]. The same behaviour is already known in literature [53,54]. This last work has been demonstrated the decreasing of Is_{50} index after 16 cycles of saline crystallization with a magnesium sulphate solution.

On Table 6, it is clear that the decreasing of Vp speed is mainly related to the mechanical strength of the rocks and, at equal cycles of T, rH and CO_2 concentration, to the salt amount (TDS) of waters used for capillary rising. In particular, it is well visible on sandstones where −8,78% △Vp is attributable to AT1 affected by rainwater. The △Vp = -16.65% on AT2 is due to the the effect of seawater. In addition, in the previous works has been demonstrated as TDS of water is directly correlated to decay in terms of loss weight for decohesion.

Assuming that the samples subjected to ageing were placed on the monument, after a hypothetical exposure of 18 years, they would present a quality VRI index always very good but the sample PC2 (Table 6).

After ageing, in fact, a great △Vp % is detected on both biomicrite samples (PC1 = -11.76% and PC2 = –23.71%). On biomicrites a Vp pre-test average of about 2860 m/s (Table 6) has been identify. Similar values in range from 3800 to 2900 m/s were shown by other measurements [55].

In biolitite samples, a lower △Vp % (PF1 = -6.79% and PF2 = -0.69%) is due to a higher mechanical strength respect than biomicrite. Pre-test Vp average value of about 5512 m/s is also in this case in agreement with [55]. Table 6 shows as the stones are characterised to values of VRI from 0.87 to 0.99. Carrara marble is the most resilient rocks due to the low porosity, permeability and hygroscopic features, with △Vp = -2.23% on MA1 and only −0.28% on MA2. High weathering resistance of Carrara marble is displayed by studies [56], measuring a △Vp = -5% after an ageing test consisting of thermal and moisture cycles. Interesting is the case of red *facies* rhyolites with △Vp IGr1 = -2.69% and △Vp IGr2 = -0.53% while the green *facies* rhyolites have △Vp IGv1 = -5.75% and △Vp IGv2 = -1.96%

Table 6
Compressional wave speed (Vp) measuring on the samples before and after the ageing with relative variation. T = temperature, rH = relative humidity, CO_2 = carbon dioxide air concentration, C_{RW} = capillary rising with rainwater, C_{SW} = capillary rising with seawater, C_{GW} = capillary rising with groundwater, C_{TW} = capillary rising with thermal water. VRI = Velocity ratio quality index. Very good = VRI > 0.95, Good = 0.75 < VRI < 0.90, Fair = 0.50 < VRI < 0.75, Poor = 0,50 < VRI < 0.25, Very poor = VRI < 0.25. Values show in this table represent the arithmetic average of 3 measurements (X, Y, Z directions).

Sample	Lithology	Reproduced conditions	Longitudinal P wave speed Vp (m/s)			VRI
			Pre test (T_T = 0 Days)	Post test (T_T = 180 Days)	△*Vp (%)*	
AT1	Sandstone	T, rH, CO_2, C_{RW}	4068 ± 608	3711 ± 638	*−8.78*	0.95 (Very good)
AT2		T, rH, CO_2, C_{SW}	4054 ± 578	3379 ± 659	*−16.65*	0.91 (Very good)
PC1	Biomicrite	T, rH, CO_2, C_{RW}	2832 ± 215	2499 ± 219	*−11.76*	0.93 (Very good)
PC2		T, rH, CO_2, C_{GW}	2889 ± 350	2204 ± 114	*–23.71*	0.87 (Good)
PF1	Biolitite	T, rH, CO_2, C_{GW}	5505 ± 328	5131 ± 442	*−6.79*	0.96 (Very good)
PF2		T, rH, CO_2, C_{RW}	5520 ± 55	5483 ± 73	*−0.69*	0.99 (Very good)
MA1	Marble	T, rH, CO_2, C_{GW}	5290 ± 242	5172 ± 128	*−2.23*	0.98 (Very good)
MA2		T, rH, CO_2, C_{RW}	5522 ± 303	5507 ± 806	*−0.28*	0.99 (Very good)
BA1	Basalt	T, rH, CO_2, C_{SW}	4988 ± 129	4707 ± 215	*−5.63*	0.97 (Very good)
BA2		T, rH, CO_2, C_{RW}	4964 ± 109	4737 ± 48	*−4.57*	0.97 (Very good)
AN1	Rhyodacite	T, rH, CO_2, C_{SW}	4621 ± 480	4435 ± 35	*−4.04*	0.98 (Very good)
AN2		T, rH, CO_2, C_{RW}	4585 ± 135	4411 ± 46	*−3.78*	0.98 (Very good)
IGv1	Rhyolite green *facies*	T, rH, CO_2, C_{TW}	2794 ± 166	2633 ± 28	*−5.75*	0.97 (Very good)
IGv2		T, rH, CO_2, C_{RW}	2808 ± 153	2753 ± 61	*−1.96*	0.99 (Very good)
IGr1	Rhyolite red *facies*	T, rH, CO_2, C_{TW}	2552 ± 118	2483 ± 27	*−2.69*	0.98 (Very good)
IGr2		T, rH, CO_2, C_{RW}	2533 ± 35	2519 ± 49	*−0.53*	0.99 (Very good)

3.3. Leeb D hardness measurements

Leeb D hardness is a typical hardness scale for metals, but it can be measured on building materials [57]. In our case, the analysis show high values of Leeb D hardness, especially on rhyodacites, basalt and marbles. Relative medium values are detected on sandstones, biolitites and rhyolites. On biomicrites, a very low hardness of 230 HLD and 240.2 HLD has been detected. Table 6 and Fig. 3 show how after ageing, both an increase and a decrease of hardness, but it is important to highlight that:

i) The decay on FITOCLIMA chamber is mainly represented by process of erosion with surface retreat (decohesion, exfoliation). Therefore, it is likely that the pre-test and post-test hardness may be referred to a different "old" stone surface than the "new fresh" post test one.

ii) The roughness of the samples surfaces that increase during the ageing due to decohesion, affects the hardness measurements, as demonstrated by other researchers [58,59].

If we assume that those two last processes are negligible in hardness modification other processes can occur during ageing.

On carbonate samples (sandstones, biomicrites, biolitites and marble), a process of calcite dissolution and formation of more soluble and less hard calcium bicarbonate $Ca(HCO_3)_2$ could be given by the equation I, in CO_2-bearing atmosphere [60]. The reverse reaction (equation II) consists of a dehydration of the same $Ca(HCO_3)_2$ with calcite secondary crystallization.

I (formation of calcium bicarbonate): $CaCO_3 + CO_2 + H_2O = Ca(HCO_3)_2$

II (dehydration of calcium bicarbonate and calcite crystallization): $Ca(HCO_3)_2 = CaCO_3 + CO_2 + H_2O$

Secondary calcite, according to the environmental condition of crystallization can have lower or higher values of porosity and hardness, respect than primary calcite (Table 7). The process of formation of calcium bicarbonate in FITOCLIMA can occur during the winter and autumn seasons, where relative humidity is higher. A consequent process of calcium bicarbonate dehydration is expected during the summers. On biomicrites an increase of hardness in an example face (Fig. 3a, b) is probably due to the formation of a "noble patina" gives by a cementation and compaction of decohesion residue on the surfaces [31,61]. This process principally occurs during the summer and dry season on FITOCLIMA.

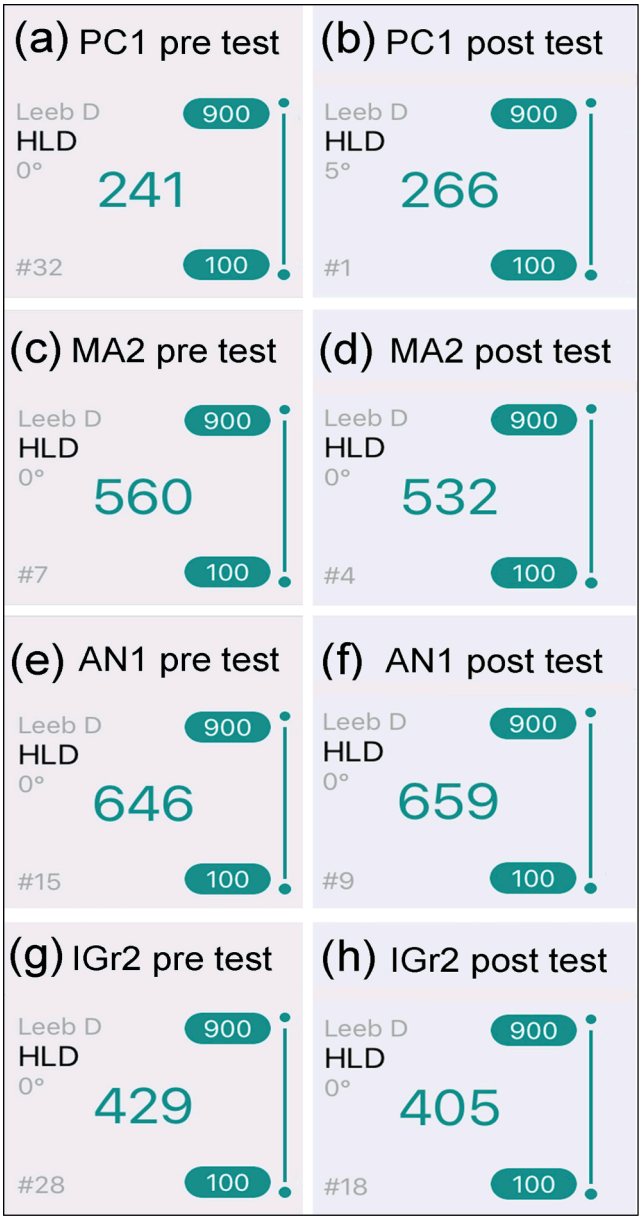

Fig. 3. Example of differences between HLD hardness measured at the centre of the faces of the cubic specimens before and after the test. (a, b) biomicrite PC1, (c, d) marble MA2, (e, f) rhyodacite AN1, (g, h) red *facies* rhyolite IGr2. The values 900–100 are referred to the maximum and minimum Hardness range measurable by the instrument. (For interpretation of the references to colour in this figure legend, the reader is referred to the web version of this article.)

Table 7
Leeb D hardness (HLD) of the samples before and after the ageing with relative variation. T = temperature, rH = relative humidity, CO_2 = carbon dioxide air concentration, C_{RW} = capillary rising with rainwater, C_{SW} = capillary rising with seawater, C_{GW} = capillary rising with groundwater, C_{TW} = capillary rising with thermal water. Values represent an arithmetic average of 6 measurements (one for each face of the cube).

Sample	Lithology	Reproduced conditions	Leeb D rebound (HLD)	Leeb D rebound (HLD)	$\triangle_{HLD}$ (%)
			Pre test (T_T = 0 days)	Post test (T_T = 180 days)	
AT1	Sandstone	T, rH, CO_2, C_{RW}	460.6 ± 58.7	432.4 ± 43.0	*−6.5*
AT2		T, rH, CO_2, C_{SW}	438 ± 47.6	493.33 ± 24.0	*12.6*
PC1	Biomicrite	T, rH, CO_2, C_{RW}	240.2 ± 4.9	250.5 ± 23.2	*4.3*
PC2		T, rH, CO_2, C_{GW}	230 ± 7.3	248.8 ± 4.9	*8.2*
PF1	Biolitite	T, rH, CO_2, C_{GW}	469.6 ± 60	512 ± 52.7	*9.0*
PF2		T, rH, CO_2, C_{RW}	506.5 ± 35.6	523.6 ± 53.9	*3.4*
MA1	Marble	T, rH, CO_2, C_{GW}	577.6 ± 18.2	545.3 ± 20.7	*−5.6*
MA2		T, rH, CO_2, C_{RW}	562.3 ± 21.1	543 ± 16.0	*−3.4*
BA1	Basalt	T, rH, CO_2, C_{SW}	632.1 ± 33.0	588.8 ± 59.5	*−6.9*
BA2		T, rH, CO_2, C_{RW}	658 ± 40.3	649.8 ± 26.5	*−1.2*
AN1	Rhyodacite	T, rH, CO_2, C_{SW}	635.6 ± 46.4	654.1 ± 62.0	*2.8*
AN2		T, rH, CO_2, C_{RW}	715.5 ± 40.2	612.8 ± 35.8	*−14.4*
IGv1	Rhyolite green *facies*	T, rH, CO_2, C_{TW}	418.3 ± 21.1	373.8 ± 31.6	*−10.6*
IGv2		T, rH, CO_2, C_{RW}	405.3 ± 18.0	369.5 ± 42.4	*−8.8*
IGr1	Rhyolite red *facies*	T, rH, CO_2, C_{TW}	412.3 ± 27.9	415.1 ± 18.8	*0.7*
IGr2		T, rH, CO_2, C_{RW}	419.6 ± 30.6	403.5 ± 17.9	*−3.8*

On some basalt, rhyodacites and rhyolites, a line corresponding to the maximum elevation of capillary rising (see model at Table 5, Fig. 2) coincides with the centre of the face, point of hardness measuring. In this line is, in fact, present a strong efflorescence deposition. In this case, a decrease of hardness (Table 7) is due to the presence of efflorescences dampening the percussion of the penetrator.

This process probably happens also on marble, where a formation of gypsum (sulphating) is also detected by diffraction (Table 4).

3.4. Gas-driven permeability measurements

The gas-driven permeability are shown in Table 8 and Fig. 4. It has been measured on sandstones, biomicrites and rhyolites. Almost all samples are characterized by a gas-driven permeability $1 < k_G < 10^4$mD classified as semipermeable (SP). Higher initial permeability is registered on sandstones AT1 and AT2 (3.5 ± 1.9D and 3.2 ± 1.8D respectively) due to a large diameter porous system in a uniform clasts framework. A wide value of water open porosity on sandstones (≈ 32%) was detected by the previous work. On biomicrites PC1 and PC2 a low value of gas-driven permeability (13.6 ± 12.2mD and 16.8 ± 12.6mD respectively) is due to a volume of clay minerals up to 15% vol., even if the porosity is up to ≈ 18%. The low permeability of biomicrite was already highlighted, indicating for this stone a hydraulic transmissivity of $1.7.10^{-3}$ m^3/s [62]. Biomicrite in outcrop and monument is characterised by a circulation of water through porosity [63].

It is interesting how a different initial permeability exists between the two chromatic *facies* of rhyolites, in particular: 2.36 ± 0.8mD, 5.3 ± 1.7mD for IGv1 and IGv2 respectively, while 39.9 ± 35.1mD, 40.1 ± 23.8mD for IGr1 and IGr2. On green rhyolites a pre-test water open porosity of 30.5% and imbibition coefficient of 18.9% were detected [31]. The same work shows a pre-test water open porosity of 32.57% and imbibition coefficient of 20.55% for red *facies* rhyolites that can, in part, have differences of permeability between *facies*. However, such a high permeability discrepancy between the two *facies* cannot only be explained with different porosity values but probably with a different tortuosity or radius of the pores.

In general, permeability of rhyolites mainly occurs by porosity and secondary fracturing. The water absorption of these rhyolites is principally due to hygroscopicity and capillarity and slightly varies according to outcrop [64]. As shown in Table 8 and Fig. 4, ageing overall determines an increase of permeability in the measured lithologies. High $\triangle k_G$ values are identified in sandstones, biomicrites and in IGv2 subjected to capillary rising with saline water. It has been observed how increasing of superficial roughness provides an increase of permeability. In addition, enlargement of micro-fractures due to salt crystallization pressure in the most superficial layers together with a modification of their tortuosity can affect the permeability value [65]. It is well visible on most erodible rocks as sandstones (Fig. 4a, b) and biomicrites (Fig. 4c, d) where k_GPC2 = 123.2% and k_GAT2 = 103.1%.

Table 8
Gas-driven permeability (k_G) of the samples before and after the ageing with relative variation.

Sample	Lithology	Reproduced conditions	Gas-driven permeability	Gas-driven permeability	$\triangle k_G$ (%)
			Pre test (T_T = 0 days)	Post test (T_T = 180 days)	
AT1	Sandstone	T, rH, CO_2, C_{RW}	3.5 ± 1.9D (SP)	6.6 ± 4.2D (SP)	*88.5*
AT2		T, rH, CO_2, C_{SW}	3.2 ± 1.8D (SP)	6.5 ± 1.5D (SP)	*103.1*
PC1	Biomicrite	T, rH, CO_2, C_{RW}	13.6 ± 12.2mD (SP)	24.9 ± 15.2mD (SP)	*83.1*
PC2		T, rH, CO_2, C_{GW}	16.8 ± 12.6mD (SP)	37.5 ± 16.2mD (SP)	*123.2*
IGv1	Rhyolite green *facies*	T, rH, CO_2, C_{TW}	2.36 ± 0.8mD (SP)	3.4 ± 2.3mD (SP)	*44.4*
IGv2		T, rH, CO_2, C_{RW}	5.3 ± 1.7mD (SP)	10.2 ± 12.9mD (SP)	*92.5*
IGr1	Rhyolite red *facies*	T, rH, CO_2, C_{TW}	39.9 ± 35.1mD (SP)	59.7 ± 17.8mD (SP)	*49.6*
IGr2		T, rH, CO_2, C_{RW}	40.1 ± 23.8mD (SP)	59.6 ± 10.2mD (SP)	*48.6*

P = permeable ($k_G > 10^4$mD), SP = semipermeable ($1 < k_G < 10^4$mD), A = arduous ($k_G < 1$mD) according to the soil and rocks permeability classification. T = temperature, rH = relative humidity, CO_2 = carbon dioxide air concentration, C_{RW} = capillary rising with rainwater, C_{SW} = capillary rising with seawater, C_{GW} = capillary rising with groundwater, C_{TW} = capillary rising with thermal water. Values represent an arithmetic average of 6 measurements (one for each face of the cube).

4. Conclusions

The accelerated ageing test outlined the physical, mechanical and morphological behaviour of materials subjected to a simulated long-term exposition to Csa climate. The test, its design and efficacy, is considered realistic since the pathologies reproduced in the climatic chamber are similar to those detected *in situ*.

The simulation and the experiment present some errors. It is important to remember how the datas of T and rH belongs to an average of two meteorological station situated about 100 km latitude distance. In addition the trends of T and rH present smooth curves that do not represent the small daily variation of the parameters. The carbon dioxide air content, constant in the climatic chamber, is subjected to daily and seasonal variations in real environment. The process of water evaporation in real environment is affected by the wind not present in FITOCLIMA. It is also important the contribution to decay given by the mechanical striking of rainwater drops/hailstorm on the sample surface. All this series of neglected decay could induce to a minor decay in climatic chamber respect than real environment.

We certainly can confirm that the information obtained by ageing can be useful for the quarry industry, architects and civil engineering. In this way, operators in the construction sector can use specific laying techniques and select the best materials to withstand specific environmental stresses. Furthermore, operators can already turn to preventive restoration technologies through water repellents, consolidants, or structural reinforcement to prevent building pathologies. Consequently, disputes that inevitably involve the waste of time, money and resources, could be avoided. The ageing, for example, highlights the decohesion problems of sandstones and biomicrites, inappropriate for buildings in marine environment. Not only, decohesion have been detected in the monuments of *Forum Traiani* and *Nora* theatre. Even if a very slow weathering has been reproduced on climatic chamber, after long exposition in natural outdoor a decay can also affects the more resilient lithologies (e.g. rhyodacites, rhyolites, basalts, biolitites). Restoration intervention at *Forum Traiani* and *Nora* theatre have been, in fact, recently documented. In particular, at *Forum Traiani* archaeological area, a deep weathering on rhyolites forced the restorers to a complete substitution of some architectural elements.

At *Nora* theatre, some restorations have only partially mitigate the weakening due to saline spray corrosion. In the same theatre, an intervention during 1979 using inappropriate coatings has accelerated the degradation processes [66,67]. The strong deterioration of the investigated materials affects the case-study monuments and entire village or cities facilities (e.g. Cagliari) located in the surroundings. Due to the higher availability, workability, and low cost of extraction, these stones were used for civil purposes in private facilities, especially at the beginning of XX Cent A.D. For these reason, degradation processes and their monitoring must be taken in account for the conservation of cities historic centres.

This accelerate ageing test with all the monitored features represents a preliminary result of a wide research. A second part will try to give found a correlation factor between simulated decay in climatic chamber and deterioration in natural outdoor.

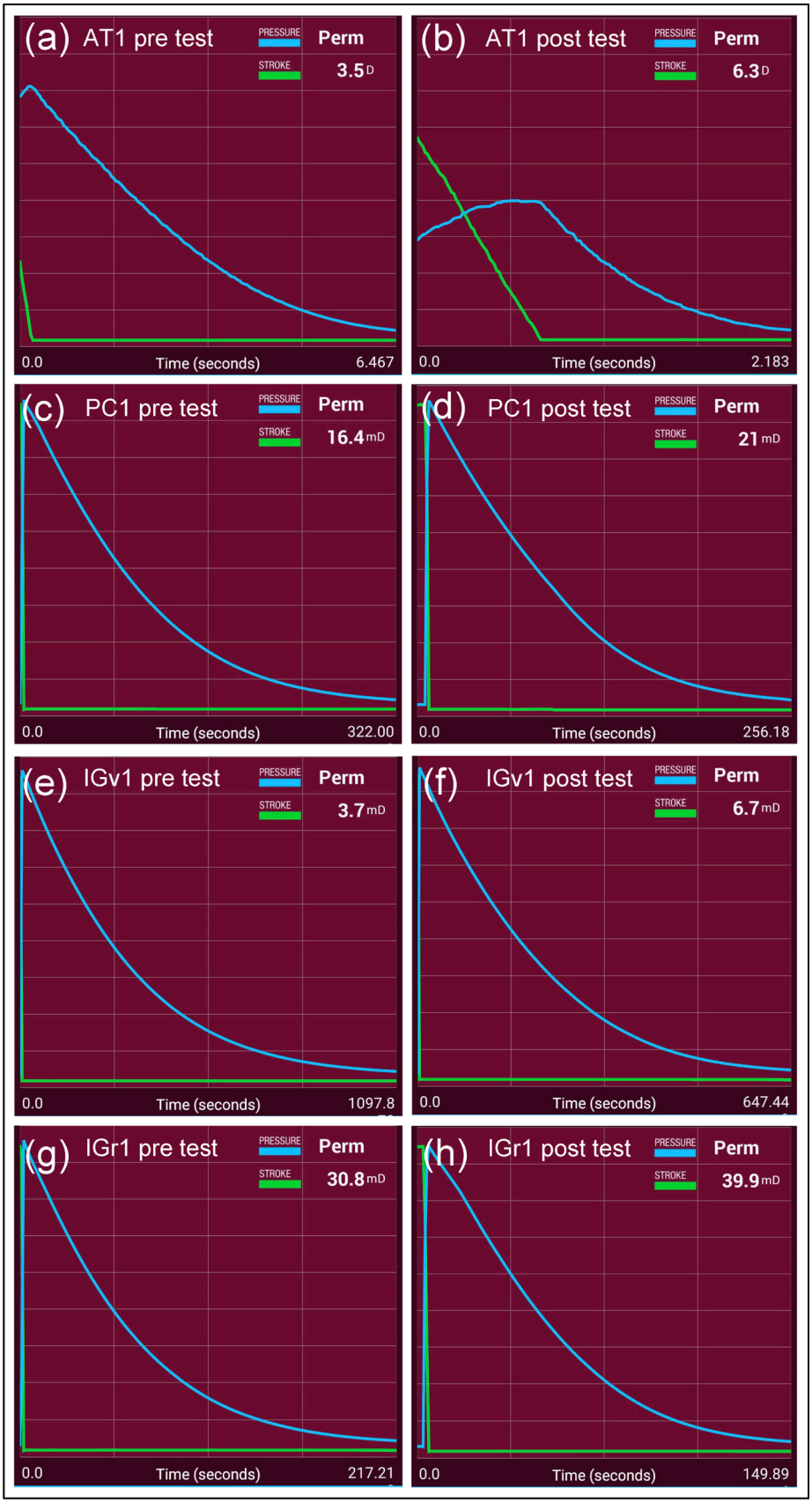

Fig. 4. Example of differences between k_G measured at the centre of the same face of cubic specimen before and after the test. (a, b) sandstones AT1, (c, d) biomicrite PC1, (e, f) rhyolite green *facies* IGv1, (g, h) rhyolite red *facies* IGr1. (For interpretation of the references to colour in this figure legend, the reader is referred to the web version of this article.)

CRediT authorship contribution statement

Fabio Sitzia: Conceptualization, Data curation, Formal analysis, Investigation, Project administration, Resources, Software, Supervision, Validation, Visualization, Writing - original draft, Writing - review & editing. **Carla Lisci:** Funding acquisition, Methodology, Validation, Visualization, Writing - review & editing. **José Mirão:** Funding acquisition, Investigation, Methodology, Validation, Visualization, Writing - review & editing.

Declaration of Competing Interest

The authors declare that they have no known competing financial interests or personal relationships that could have appeared to influence the work reported in this paper.

Acknowledgements

Fabio Sitzia gratefully acknowledges Sardinian Regional Government for the financial support of his PhD scholarship (P.O.R. Sardegna F. S.E. – Operational Programme of the Autonomous Region of Sardinia, European Social Fund 2014-2020 – Axis III Education and training, Thematic goal 10, Investment Priority 10ii), Specific goal 10.5.

The authors gratefully acknowledge the following funding sources: ColourStone—Colour of commercial marbles and limestone: causes and changings (ALT20-03-0145-FEDER-000017) and INOVSTONE4.0 (POCI-01-0247-FEDER-024535), co-financed by the European Union through the European Regional Development Fund (FEDER) and Fundação para a Ciência e Tecnologia (FCT) under the project UID/Multi/04449/2013 (POCI-01-0145- FEDER-007649).

References

[1] C. Lisci, F. Sitzia, Degrado, danni e difetti delle pietre naturali e dei laterizi. Meccanismi di alterazione, patologie, tecniche diagnostiche e scehde pratiche, Maggioli, 2021.
[2] H.J. Porck, Rate of paper degradation the predictive value of artificial aging tests, Preservation. (2000).
[3] M. Crewdson, Outdoor weathering must verify accelerated testing, in: Annu. Tech. Conf. - ANTEC, Conf. Proc., 2011.
[4] M.J. Crewdson, W.D. Ketola, Best practices in weathering: outdoor and accelerated testing compared, Eur. Coatings J., 2009.
[5] UNI EN 13919:2004 Natural stone test methods - determination of resistance to ageing by SO2 action in the presence of humidity., n.d.
[6] UNI EN 12370:2001 Natural stone test methods - determination of resistance to salt crystallisation, n.d.
[7] UNI EN 14066:2013 Natural stone test methods - determination of resistance to ageing by thermal shock, n.d.
[8] UNI EN 14147:2005 Natural stone test methods - determination of resistance to ageing by salt mist, (n.d.).
[9] UNI EN 12371:2010 Natural stone test methods - determination of frost resistance, n.d.
[10] DIN 50017 Condensation water test atmospheres, n.d.
[11] DIN 50018 Testing in a saturated atmosphere in the presence of sulfur dioxide, n.d.
[12] DIN 50021 Spray tests with different sodium chloride solutions, n.d.
[13] ISO 9227:2017 Corrosion tests in artificial atmospheres - salt spray tests, n.d.
[14] ASTM G154 C.7 Accelerated Weathering (QUV), n.d.
[15] M. Takarli, W. Prince, R. Siddique, Damage in granite under heating/cooling cycles and water freeze-thaw condition, Int. J. Rock Mech. Min. Sci. 45 (7) (2008) 1164–1175, https://doi.org/10.1016/j.ijrmms.2008.01.002.
[16] R. Altindag, I.S. Alyildiz, T. Onargan, Mechanical property degradation of ignimbrite subjected to recurrent freeze–thaw cycles, Int. J. Rock Mech. Min. Sci. 41 (6) (2004) 1023–1028, https://doi.org/10.1016/j.ijrmms.2004.03.005.
[17] M. Fener, I. İnce, Effects of the freeze-thaw (F-T) cycle on the andesitic rocks (Sille-Konya/Turkey) used in construction building, J. African Earth Sci. 109 (2015) 96–106, https://doi.org/10.1016/j.jafrearsci.2015.05.006.
[18] S. Siegesmund, K. Ullemeyer, T. Weiss, E.K. Tschegg, Physical weathering of marbles caused by anisotropic thermal expansion, Int. J. Earth Sci. 89 (1) (2000) 170–182, https://doi.org/10.1007/s005310050324.
[19] M. Mutlutürk, R. Altindag, G. Türk, A decay function model for the integrity loss of rock when subjected to recurrent cycles of freezing-thawing and heating-cooling, Int. J. Rock Mech. Min. Sci. 41 (2) (2004) 237–244, https://doi.org/10.1016/S1365-1609(03)00095-9.
[20] F. Sitzia, Monitoraggio del degrado e conservazione del Patrimonio monumentale della Regione Sardegna attraverso caratterizzazione geochimica, petrofisica e micro-fotogrammetrica di superfici lapidee, University of Cagliari, 2019.
[21] V. Cárdenes, F.J. Mateos, S. Fernández-Lorenzo, Analysis of the correlations between freeze-thaw and salt crystallization tests, Environ. Earth Sci. 71 (3) (2014) 1123–1134, https://doi.org/10.1007/s12665-013-2516-7.
[22] H.H. Selim, A. Karakaş, Ö. Coruk, Investigation of engineering properties for usability of Lefke stone (Osmaneli/Bilecik) as building stone, Bull. Eng. Geol. Environ. 78 (8) (2019) 6047–6059, https://doi.org/10.1007/s10064-019-01520-3.
[23] M.R. Velosa, A.L., VEIGA, Development of artificial ageing tests for renders - Application to conservation mortars., in: T. G. (Ed.), Proceeding 7th Int. Mason. Conf., 2006.
[24] A. Arizzi, H. Viles, G. Cultrone, Experimental testing of the durability of lime-based mortars used for rendering historic buildings, Constr. Build. Mater. 28 (1) (2012) 807–818, https://doi.org/10.1016/j.conbuildmat.2011.10.059.
[25] R. Geiger, Classificação climática de Köppen- Geiger, Creat. Commons Attrib. Alike 3.0 Unported. (1936).
[26] M. Labus, J. Bochen, Sandstone degradation: an experimental study of accelerated weathering, Environ. Earth Sci. 67 (7) (2012) 2027–2042, https://doi.org/10.1007/s12665-012-1642-y.
[27] V. Kočí, J. Maděra, J. Fořt, J. Žumár, M. Pavlíková, Z. Pavlík, R. Černý, Service life assessment of historical building envelopes constructed using different types of sandstone: a computational analysis based on experimental input data, Sci. World J. 2014 (2014) 1–12, https://doi.org/10.1155/2014/802509.
[28] J. Bochen, Assessment of building materials exposed to atmosphere agents by testing in simulated environment, Archit. Civ. Eng. Environ. 1 (2013) 17–26.
[29] A. Chabas, A. Fouqueau, M. Attoui, S.C. Alfaro, A. Petitmangin, A. Bouilloux, M. Saheb, A. Coman, T. Lombardo, N. Grand, P. Zapf, R. Berardo, M. Duranton, R. Durand-Jolibois, M. Jerome, E. Pangui, J.J. Correia, I. Guillot, S. Nowak, Characterisation of CIME, an experimental chamber for simulating interactions between materials of the cultural heritage and the environment, Environ. Sci. Pollut. Res. 22 (23) (2015) 19170–19183, https://doi.org/10.1007/s11356-015-5083-5.
[30] T. Wells, P. Binning, G. Willgoose, G. Hancock, Laboratory simulation of the salt weathering of schist: I. Weathering of schist blocks in a seasonally wet tropical environment, Earth Surf. Process. Landforms. (2006), https://doi.org/10.1002/esp.1248.
[31] F. Sitzia, C. Lisci, J. Mirão, Accelerate ageing on building stone materials by simulating daily, seasonal thermo-hygrometric conditions and solar radiation of Csa mediterranean climate, Constr. Build. Mater. 266 (2021) 121009, https://doi.org/10.1016/j.conbuildmat.2020.121009.
[32] S. Columbu, F. Antonelli, F. Sitzia, Origin of Roman worked stones from St. Saturno christian Basilica (south Sardinia, Italy), Mediterr. Archaeol. Archaeom. 18 (2018), https://doi.org/10.5281/zenodo.1256047.
[33] S. Columbu, C. Lisci, F. Sitzia, G. Buccellato, Physical–mechanical consolidation and protection of Miocenic limestone used on mediterranean historical monuments: the case study of Pietra Cantone (southern Sardinia, Italy), Environ. Earth Sci. 76 (4) (2017), https://doi.org/10.1007/s12665-017-6455-6.
[34] S. Columbu, A. Gioncada, M. Lezzerini, F. Sitzia, Mineralogical-chemical alteration and origin of ignimbritic stones used in the old cathedral of nostra Signora di Castro (Sardinia, Italy), Stud. Conserv. 64 (7) (2019) 397–422, https://doi.org/10.1080/00393630.2018.1565016.
[35] S. Columbu, Petrographic and geochemical investigations on the volcanic rocks used in the Punic-Roman archaeological site of Nora (Sardinia, Italy), Environ. Earth Sci. 77 (16) (2018), https://doi.org/10.1007/s12665-018-7744-4.
[36] S. Fabio, B. Massimo, C. Stefano, L. Carla, M. Catarina, M. José, Ancient restoration and production technologies of Roman mortars from monuments placed in hydrogeological risk areas: a case study, Archaeol. Anthropol. Sci. 12 (7) (2020), https://doi.org/10.1007/s12520-020-01080-8.
[37] S. Kahraman, U. Ulker, M.S. Delibalta, A quality classification of building stones from P-wave velocity and its application to stone cutting with gang saws, J. South. African Inst. Min. Metall. (2007), https://doi.org/10.3997/2214-4609-pdb.26.o5-06.
[38] SO 16859-2:2015 Metallic materials - Leeb hardness test - Part 2: Verification and calibration of the testing devices, n.d.
[39] H. Bansa, Accelerated aging of paper: Some ideas on its practical benefit, Restaurator. 23 (2002) 106–117.
[40] H. Bansa, Accelerated aging tests in conservation research: some ideas for a future method, Restaurator. (1992), https://doi.org/10.1515/rest.1992.13.3.114.
[41] B. Buttervort, The recording comparison and use of outdoor exposure test, Trans. J. Br. Ceram. Soc. 63 (1964).
[42] M. Prokop, Accelerated tests on durability ageing of elevation materials, Mater. Bodowlane. 10 (1999).
[43] K. Motohoshi, T. Nireki, Investigation into degradation mechanisc for masonry coating systems by microscopic analysis methods, in: III Int. Conf. Durab. Build. Mater. Components VTT Symp. Espoo, 1984: pp. 241–253.
[44] F. Staffa, M. Testa, G. Uras, Evaluation of groundwater quality in the Wide Urban Area of Cagliari (Southern Sardinia - Italy), Rend. Online Soc. Geol. Ital. 3 (2008) 740–741.
[45] K.J. Stanienda-Pilecki, Magnesium calcite in muschelkalk limestones of the polish part of the Germanic Basin, Carbonates and Evaporites. 33 (4) (2018) 801–821, https://doi.org/10.1007/s13146-018-0437-y.
[46] E. Ruiz-Agudo, F. Mees, P. Jacobs, C. Rodriguez-Navarro, The role of saline solution properties on porous limestone salt weathering by magnesium and sodium sulfates, Environ. Geol. 52 (2) (2007) 269–281, https://doi.org/10.1007/s00254-006-0476-x.
[47] S. Columbu, M. Marchi, R. Martorelli, M. Palomba, F. Pinna, F. Sitzia, L. Tanzini, A. Virdis, Architettura romanica e territorio, CUEC, Cagliari, 2018.

[48] M. Murgia, Petrographic and petrophysical characterization of the volcanic stones used in the construction of some Romanesque churches in central-northern Sardinia, 2014, University of Cagliari.
[49] P.M. Driessen, R. Schoorl, Mineralogy and morphology of salt efflorescences on saline soils in the great konya basin, Turkey, J. Soil Sci., 1973, https://doi.org/10.1111/j.1365-2389.1973.tb02310.x.
[50] B. Dettori, R.A. Zanzari, P. Zuddas, Le acque termali della Sardegna. PFE Sottoprogetto Energia Geotermica. Relazione finale sul tema della ricerca: Studi geologici e geofisici finalizzati alla ricerca di fluidi caldi nel sottosuolo., 1982.
[51] D. Bionda, RUNSALT - A graphical user interface to the ECOS thermodynamic model for the prediction of the behaviour of salt mixtures under changing climate conditions. http://science.sdf-eu.org/runsalt/, 2005.
[52] C.A. Price, An expert chemical model for determining the environmental conditions needed to prevent salt damage in porous materials, 2000, London.
[53] E. Molina, G. Cultrone, E. Sebastián, F.J. Alonso, Evaluation of stone durability using a combination of ultrasound, mechanical and accelerated aging tests, J. Geophys. Eng. 10 (3) (2013) 035003, https://doi.org/10.1088/1742-2132/10/3/035003.
[54] M. Heidari, A.A. Momeni, F. Naseri, New weathering classifications for granitic rocks based on geomechanical parameters, Eng. Geol. 166 (2013) 65–73, https://doi.org/10.1016/j.enggeo.2013.08.007.
[55] S. Fais, F. Cuccuru, P. Ligas, G. Casula, M.G. Bianchi, Integrated ultrasonic, laser scanning and petrographical characterisation of carbonate building materials on an architectural structure of a historic building, Bull. Eng. Geol. Environ. 76 (1) (2017) 71–84, https://doi.org/10.1007/s10064-015-0815-9.
[56] R. Bellopede, E. Castelletto, B. Schouenborg, P. Marini, Assessment of the European Standard for the determination of resistance of marble to thermal and moisture cycles: recommendations for improvements, Environ. Earth Sci. 75 (11) (2016), https://doi.org/10.1007/s12665-016-5748-5.
[57] M. Gomez-Heras, D. Benavente, C. Pla, J. Martinez-Martinez, R. Fort, V. Brotons, Ultrasonic pulse velocity as a way of improving uniaxial compressive strength estimations from Leeb hardness measurements, Constr. Build. Mater. 261 (2020) 119996, https://doi.org/10.1016/j.conbuildmat.2020.119996.
[58] J. Desarnaud, K. Kiriyama, B. Bicer Simsir, K. Wilhelm, H. Viles, A laboratory study of Equotip surface hardness measurements on a range of sandstones: What influences the values and what do they mean? Earth Surf Process. Landforms. 44 (7) (2019) 1419–1429, https://doi.org/10.1002/esp.v44.710.1002/esp.4584.
[59] K. Wilhelm, H. Viles, Ó. Burke, Low impact surface hardness testing (Equotip) on porous surfaces – advances in methodology with implications for rock weathering and stone deterioration research, Earth Surf. Process. Landforms. 41 (8) (2016) 1027–1038, https://doi.org/10.1002/esp.v41.810.1002/esp.3882.
[60] C.S. Adams, A.C. Swinnerton, Solubility of limestone, Eos Trans. Am. Geophys. Union. 18 1937 504 508, https://doi.org/https://doi.org/10.1029/TR018i002p00504.
[61] J. Delgado Rodrigues, Stone patina. A controversial concept of relevant importance in conservation, Int. Semin. Theory Pract. Conserv. a Tribut. to Cesare Brand, 2006.
[62] A. Pala, Carta idrogeologica di Cagliari, Coedisar, Cagliari, 1997.
[63] C. Atzeni, S. Cara, U. Sanna, G. Sistu, Restauro dell ' edilizia storica della citta di Cagliari : i I ruolo della caratterizzazione dei material i calcarei delle antiche cave, Kermes. 10 (1991) 9–15.
[64] S. Argiolas, G. Carcangiu, D. Floris, L. Massidda, P. Meloni, A Vernier e piroclastiti dell'antica Forum Traiani (Fordongianus), Sardegna Centrale: caratterizzazione, tecniche di estrazione, e specificità di utilizzo nel corso dei secoli, In Le risorse lapidee dall'antichità ad oggi in area mediterranea., in: LE RISORSE LAPIDEE DALL'ANTICHITÀ AD OGGI AREA Mediterr 2006 Torino 33 38.
[65] A. Akhavan, S.-M.-H. Shafaatian, F. Rajabipour, Quantifying the effects of crack width, tortuosity, and roughness on water permeability of cracked mortars, Cem. Concr. Res. 42 (2) (2012) 313–320, https://doi.org/10.1016/j.cemconres.2011.10.002.
[66] L. Massidda, U. Sanna, La cristallizzazione salina nei materiali da costruzione, L'esempio del sito archeologico di Nora, Sardegna, 1994.
[67] L. Massidda, C. Atzeni, U. Sanna, Acquisizione di dati su processi di degrado e interventi di consolidamento alle terme a mare di Nora (Pula, CA). Relazione finale della convenzione/contratto del 18–07-1994 stipulata con la soprintendenza archeologica per le provincie di Cagliari ed Orist, 1994.